Multi-Label Learning with Regularization Enriched Label-Specific Features

Ze-Sen Chen CHENZS@SEU.EDU.CN
Min-Ling Zhang ZHANGML@SEU.EDU.CN
School of Computer Science and Engineering, Southeast University, Nanjing 210096, China
Key Laboratory of Computer Network and Information Integration (Southeast University), Ministry of Education, China

Editors: Wee Sun Lee and Taiji Suzuki

Abstract

Multi-label learning learns from examples each associated with multiple class labels simultaneously, and the goal is to induce a predictive model which can assign a set of relevant labels for the unseen instance. Label-specific features serve as an effective strategy towards inducing multi-label predictive model, where the relevancy of each class label is determined by employing tailored features encoding inherent and distinct characteristics of the class label its own. In this paper, a regularization based approach named REEL is proposed for label-specific features generation, which works by enriching label-specific feature representation for each class label via synergizing informative label-specific features from other class labels with sparse regularization. Specifically, full-order label correlations are considered by REEL while the number of classifiers induced for multi-label prediction is linear to the number of class labels. Extensive experiments on fifteen benchmark multi-label data sets clearly show the favorable performance of REEL against other state-of-the-art multi-label learning approaches with label-specific features.

Keywords: Multi-label, Label-specific features, Sparse regularization

1. Introduction

Multi-label learning deals with objects with rich semantics where each example is represented by a single instance (feature vector) while associated with multiple class labels simultaneously (Zhang and Zhou, 2014; Gibaja and Ventura, 2015). In recent years, the need to learn from multi-label examples are widely witnessed in various applications such as text classification (Rubin et al., 2012), image annotation (Sun et al., 2014), social network analysis (Wang and Sukthankar, 2013), music emotion categorization (Trohidis et al., 2011; Wu et al., 2014), bioinformatics (Pan et al., 2019), etc.

To learn from multi-label examples, one common strategy is to build predictive model based on the single instance representation to discriminate all the class labels (Zhang and Zhou, 2014; Gibaja and Ventura, 2015). Nonetheless, the inherent and distinct characteristics of each class label is not fully considered by employing identical feature representation for model induction. For instance, in text categorization, features corresponding to word terms *election*, *debate* and *voting* are informative in discriminating political and non-political documents, while features corresponding to word terms *Olympics*, *championship* and *referee* are informative in discriminating sports and non-sports documents. Therefore, the strategy of *label-specific features* has been proposed to facilitating multi-label learning which aims to determine the relevancy of each class label with tailored features of its own.

Existing attempts towards label-specific features work by generating tailored features for each class label independently (Zhang and Wu, 2015; Xu et al., 2016), considering pairwise label correlations (Huang et al., 2018; Weng et al., 2018), or selecting a subset of features from the original feature space (Huang et al., 2016; Sun et al., 2016; Zhang et al., 2018b). To generate label-specific features with strong discriminative abilities for inducing multi-label predictive model, it is desirable that the correlations among class labels can be fully exploited. On the other hand, the computational cost for generating label-specific features should be manageable especially in terms of the number of class labels in label space.

In this paper, a novel approach named REEL, i.e. *REgularization Enriched Label-specific features*, is proposed to learning from multi-label examples. Briefly, REEL employs a two-stage procedure for label-specific features generation. In the first stage, a number of base label-specific features are constructed by conducting clustering analysis on the positive and negative instances of each class label (Zhang and Wu, 2015; Xu et al., 2016). After that, REEL enriches the label-specific feature representation for each class label via synergizing informative base label-specific features from other class labels with sparse regularization. Thereafter, a set of binary classification models are induced based on the enriched label-specific features to determine the relevancy of each class label for unseen instance. Comprehensive experiments across a total of fifteen benchmark data sets validate the superior performance of REEL against state-of-the-art multi-label learning approaches based on label-specific features.

The rest of this paper is organized as follows. In Section 2, related works on label-specific features are briefly reviewed. In Section 3, technical details of the proposed approach based on label-specific features are presented. In Section 4, experimental results of comparative studies are reported. Finally, Section 5 concludes.

2. Related Work

The task of multi-label learning has been extensively studied in recent years, where significant number of approaches have been proposed to learning from examples with multiple class labels simultaneously (Zhang and Zhou, 2014; Gibaja and Ventura, 2015). Due to the combinatorial nature of the label set to be predicted, most works focus on exploiting correlations among class labels to help induce the multi-label predictive model. Generally speaking, the order of label correlations considered by the learning algorithm can be *first-order* where the multi-label learning problem is tacked by treating each class label independently (Boutell et al., 2004; Zhang et al., 2018c), *second-order* where the multi-label learning problem is tackled by modeling pairwise interactions between class labels (Fürnkranz et al., 2008; Brinker et al., 2014), or *high-order* where the multi-label learning problem is tackled by considering high-order interactions among a subset of or all class labels (Read et al., 2011; Tsoumakas et al., 2011).

In addition to the exploitation of label correlations, the generalization performance of multi-label learning system can be improved by manipulating the feature space. The most straightforward feature manipulation strategy is to conduct dimensionality reduction (Sun et al., 2013) or feature selection (Pereira et al., 2018) over the original feature space. Other feature manipulation strategies include generating meta-level features by extracting refined discriminative information from the original features (Yang and Gopal, 2012; Canuto et al., 2016) and making use of multi-view representation for multi-label data (Zhu et al., 2016; Zhan and Zhang, 2017; Zhang et al., 2018a). Nonetheless, these feature manipulation strategies share the same mechanism of using identical feature representation in the discrimination processes of all class labels.

In contrast to the above strategies for multi-label feature manipulation, the strategy of label-specific features works by utilizing tailored feature representation for each class label to better characterize its inherent and distinct properties. For label-specific features generation, one can conduct clustering analysis (Zhang and Wu, 2015) or attribute reduction (Xu et al., 2016) on the positive and negative instances of each class label independently. To consider label correlations in the generation procedure of label-specific features, it is not difficult to incorporate pairwise label correlations with similarity measure between class labels (Huang et al., 2018) or nearest neighbor rule (Weng et al., 2018). Rather than representing the label-specific features in the transformed feature space, it is also feasible to work with the original feature space by retaining a different subset of original features for each class label (Huang et al., 2016; Zhang et al., 2018b) or a group of class labels (Sun et al., 2016).

3. The REEL Approach

Let $\mathcal{X} = \mathbb{R}^d$ be the d-dimensional feature space and $\mathcal{Y} = \{l_1, l_2, \ldots, l_q\}$ be the label space consisting of q possible class labels. Given the multi-label training set $\mathcal{D} = \{(\boldsymbol{x}_i, Y_i) | 1 \leq i \leq m\}$, where $\boldsymbol{x}_i = [x_{i1}, x_{i1}, ..., x_{id}]^\top$ is a d-dimensional feature vector and $Y_i \subseteq \mathcal{Y}$ is the set of relevant labels associated with $\boldsymbol{x}_i$. The task of multi-label learning is to induce a multi-label predictor $h : \mathcal{X} \mapsto 2^{\mathcal{Y}}$ which maps from the feature space to the powerset of label space.

Based on the strategy of label-specific features, REEL works by generating a feature mapping $\psi_k : \mathcal{X} \mapsto \mathcal{Z}_k$ for each class label l_k $(1 \leq k \leq q)$. Thereafter, a binary classification model $g_k : \mathcal{Z}_k \mapsto [0, 1]$ is induced based on the mapped feature space $\mathcal{Z}_k$. Accordingly, for the unseen instance $\boldsymbol{x} \in \mathcal{X}$, its label set can be predicted as $h(\boldsymbol{x}) = \{l_k \mid g_k(\psi_k(\boldsymbol{x})) \geq 0.5,\ 1 \leq k \leq q\}$. Specifically, REEL employs a two-stage procedure to fulfill the task of label-specific features generation.

For each class label $l_k \in \mathcal{Y}$, we can divide the instances into positive and negative set, following the clustering mechanism to analyze structural information of input space (Zhang and Wu, 2015; Xu et al., 2016), REEL adopts k-means algorithm to partition both set into N_k clusters with:

$$N_k = r \cdot \begin{cases} |l_k \in Y_k|, & \text{if } |l_k \in Y_k| < |l_k \notin Y_k| \\ |l_k \notin Y_k|, & \text{otherwise} \end{cases} \tag{1}$$

Here, the clustering centroids are denoted as $\{\boldsymbol{p}_1^k, \boldsymbol{p}_2^k, \ldots, \boldsymbol{p}_{N_k}^k\}$ and $\{\boldsymbol{n}_1^k, \boldsymbol{n}_2^k, \ldots, \boldsymbol{n}_{N_k}^k\}$ respectively.

Accordingly, the $2N_k$-dimensional base label-specific features $\phi_k : \mathcal{X} \mapsto \mathbb{R}^{2N_k}$ can be generated by querying the distance between the instance and clustering centroids:

$$\phi_k(\boldsymbol{x}) = [d(\boldsymbol{x}, \boldsymbol{p}_1^k), \ldots, d(\boldsymbol{x}, \boldsymbol{p}_{N_k}^k), d(\boldsymbol{x}, \boldsymbol{n}_1^k), \ldots, d(\boldsymbol{x}, \boldsymbol{n}_{N_k}^k)]^\top \tag{2}$$

Here, $d(\cdot, \cdot)$ returns the Euclidean distance between two feature vectors.

After having the base label-specific features in the first stage, REEL aims to enrich the label-specific features for each class label by exploiting its correlations with the other class labels. For each class label $l_k \in \mathcal{Y}$, let $\boldsymbol{y}_k = [y_{k1}, y_{k2}, \ldots, y_{km}]^\top$ denote the labeling vector for l_k where

Table 1: The pseudo-code of REEL

```
Inputs:
$\mathcal{D}$:  multi-label training set $\{(\boldsymbol{x}_i, Y_i) \mid 1 \leq i \leq m\}$
     $(\boldsymbol{x}_i \in \mathcal{X}, Y_i \subseteq \mathcal{Y}, \mathcal{X} = \mathbb{R}^d, \mathcal{Y} = \{l_1, l_2, \ldots, l_q\})$
$\lambda$:  the regularization parameter ($\lambda > 0$)
$\mathcal{L}$:  the binary learning algorithm
$\boldsymbol{x}$:  the unseen instance ($\boldsymbol{x} \in \mathcal{X}$)

Outputs:
$Y$:  predicted label set for $\boldsymbol{x}$

Process:
for $k = 1$ to $q$ do
    Perform $k$-means algorithm on positive and negative set for $l_k$ to obtain the clustering centroids $\{\boldsymbol{p}_1^k, \boldsymbol{p}_2^k, \ldots, \boldsymbol{p}_{N_k}^k\}$ and $\{\boldsymbol{n}_1^k, \boldsymbol{n}_2^k, \ldots, \boldsymbol{n}_{N_k}^k\}$ respectively, where $N_k$ is set according to Eq.(1);
    Form the base label-specific feature mapping $\phi_k$ for $l_k$ according to Eq.(2);
end for
for $k = 1$ to $q$ do
    Solve the $L_1$-regularized optimization problem Eq.(4) (along with Eq.(3)) to obtain the weight vector $\boldsymbol{\beta}_k$;
    Form the final label-specific feature mapping $\psi_k$ according to Eq.(5) and Eq.(6);
end for
for $k = 1$ to $q$ do
    Generate the binary training set $\mathcal{D}_k$ for $l_k$ according to Eq.(7);
    Induce the binary classifier $g_k$ for $l_k$ by invoking $\mathcal{L}$ on $\mathcal{D}_k$: $g_k \leftarrow \mathcal{L}(\mathcal{D}_k)$;
end for
Obtain the prediction vector $\boldsymbol{\eta}$ for $\boldsymbol{x}$ by querying binary classifiers $g_k$ $(1 \leq k \leq q)$;
Update $\boldsymbol{\eta}$ to $\hat{\boldsymbol{\eta}}$ according to Eq.(8) and Eq.(9);
Return $Y = \{l_k \mid \hat{\eta}_k \geq 0.5,\ 1 \leq k \leq q\}$.
```

$y_{ki} = 1$ if $l_k \in Y_i$ and $y_{ki} = 0$ otherwise. Furthermore, let $\varphi_k(\boldsymbol{x})$ denote the d_k-dimensional feature vector formed by concatenating all base label-specific features from all class labels other than l_k:

$$\varphi_k(\boldsymbol{x}) = [\phi_1(\boldsymbol{x}), ..., \phi_{k-1}(\boldsymbol{x}), \phi_{k+1}(\boldsymbol{x}), ..., \phi_q(\boldsymbol{x})]^\top \tag{3}$$

Here, $d_k = \sum_{k' \neq k} 2m_{k'}$. Let $\mathbf{X}_k = [\varphi_k(\boldsymbol{x}_1), \varphi_k(\boldsymbol{x}_2), \ldots, \varphi_k(\boldsymbol{x}_m)]^\top$ be the $m \times d_k$ matrix formed by applying ϕ_k to all training examples, the correlation between l_k and the other class labels are modeled by solving the following optimization least-squares optimization problem with sparse regularization:

$$\min_{\boldsymbol{\beta}_k \in \mathbb{R}^{d_k}} \quad ||\boldsymbol{y}_k - \mathbf{X}_k \cdot \boldsymbol{\beta}_k||_2^2 + \lambda \cdot ||\boldsymbol{\beta}_k||_1 \tag{4}$$

Here, $\boldsymbol{\beta}_k = [\beta_{k1}, \beta_{k2}, \ldots, \beta_{kd_k}]^\top$ is the weight vector to be optimized whose elements encode the importance of features in φ_k in predicting the relevancy of l_k. Furthermore, $\lambda > 0$ corresponds to the regularization parameter. After solving the above problem with off-the-shelf sparse regression techniques, REEL identifies base label-specific features from other class labels which can be used to enrich ϕ_k by thresholding the learned weight vector $\boldsymbol{\beta}_k$. Specifically, let $\mathcal{I}_k$ stores the indices of features in φ_k whose corresponding weight has magnitude greater than the threshold γ:

$$\mathcal{I}_k = \{a \mid |\beta_{ka}| \geq \gamma,\ 1 \leq a \leq d_k\} \tag{5}$$

Then, the final label-specific features $\psi_k : \mathcal{X} \mapsto \mathcal{Z}_k$ for l_k are generated as:

$$\psi_k(\boldsymbol{x}) = [\phi_k(\boldsymbol{x}), \Pi_{\mathcal{I}_k}(\varphi_k(\boldsymbol{x}))] \tag{6}$$

Here, $\Pi_{\mathcal{I}}(\boldsymbol{u})$ represents the projection operation of retaining features in the index set $\mathcal{I}$ for $\boldsymbol{u}$. Therefore, the dimensionality of $\mathcal{Z}_k$ corresponds to $2N_k + |\mathcal{I}_k|$.

To train the predictive model, a binary training set $\mathcal{D}_k$ for l_k can be transformed from the original multi-label training set $\mathcal{D}$ as follows:

$$\mathcal{D}_k = \{(\psi_k(\boldsymbol{x}_i), y_{ki}) \mid 1 \leq i \leq m\} \tag{7}$$

Then, a binary classification model $g_k : \mathcal{Z}_k \mapsto [0,1]$ can be induced from $\mathcal{D}_k$ by invoking some binary learning algorithm $\mathcal{L}$: $g_k \leftarrow \mathcal{L}(\mathcal{D}_k)$. For unseen instance $\boldsymbol{x} \in \mathcal{X}$, let $\boldsymbol{\eta} = [\eta_1, \eta_2, \ldots, \eta_q]^\top = [g_1(\psi_1(\boldsymbol{x})), g_2(\psi_2(\boldsymbol{x})), \ldots, g_q(\psi_q(\boldsymbol{x}))]^\top$ denote the prediction vector yielded by the induced binary classifiers. Instead of determining the relevancy of each class label for $\boldsymbol{x}$ based on $\boldsymbol{\eta}$, i.e. $h(\boldsymbol{x}) = \{l_k \mid \eta_k \geq 0.5,\ 1 \leq k \leq q\}$, REEL improves $\boldsymbol{\eta}$ by further considering correlations among class labels.

Let $\hat{\boldsymbol{y}}_k = [\hat{y}_{k1}, \hat{y}_{k2}, \ldots, \hat{y}_{km}]^\top$ denote the signed labeling vector with $\hat{y}_{ki} = +1$ if $l_k \in Y_i$ and $\hat{y}_{ki} = -1$ otherwise. Then, the correlation matrix $\boldsymbol{\Theta} = [\theta_{jk}]_{q \times q}$ is set according to the cosine similarity between the signed labeling vectors:

$$\forall\, 1 \leq j,k \leq q: \quad \theta_{jk} = \frac{\hat{\boldsymbol{y}}_j^\top \cdot \hat{\boldsymbol{y}}_k}{||\hat{\boldsymbol{y}}_j||_2 \cdot ||\hat{\boldsymbol{y}}_k||_2} \tag{8}$$

Conceptually, θ_{jk} takes the value within $[-1,+1]$ whose magnitude reflects the strength of correlation (either positive or negative) between l_j and l_k. The correlation matrix $\boldsymbol{\Theta}$ is updated by thresholding θ_{jk} into zero if its correlation strength is not strong, i.e. $|\theta_{jk}| < \sigma$.[1]

By utilizing the correlation matrix $\boldsymbol{\Theta}$, the prediction vector $\boldsymbol{\eta}$ is updated to $\hat{\boldsymbol{\eta}}$ with:

$$\hat{\eta}_k = \begin{cases} \sum_{j=1}^{q} \theta_{jk} \cdot \eta_j, & \text{if } \left|\sum_{j=1}^{q} \theta_{jk} \cdot \eta_j\right| > \sigma \text{ or} \\ & \left|\sum_{j=1}^{q} \theta_{jk} \cdot \eta_j\right| < 1 - \sigma \\ \eta_k, & \text{otherwise} \end{cases} \tag{9}$$

Table 1 summarizes the complete procedure of REEL. In the first stage, the base label-specific features are generated by conducting clustering analysis on the positive and negative instances of each class label (Steps 1-4). In the second stage, the final label-specific features are generated

[1] In this paper, the thresholding parameters γ (Eq.(5)) and σ are fixed to be 0.2 and 0.9 respectively. Furthermore, the ratio parameter r in Eq.(1) is fixed to be 0.1 (Zhang and Wu, 2015).

Table 2: Characteristics of the multi-label experimental data sets.

Data set	$\lvert\mathcal{S}\rvert$	$dim(\mathcal{S})$	$L(\mathcal{S})$	$F(\mathcal{S})$	$LCard(\mathcal{S})$	$LDen(\mathcal{S})$	$DL(\mathcal{S})$	$PDL(\mathcal{S})$	Domain
Cal500	502	68	174	numeric	26.044	0.150	502	1.000	audio
emotions	593	72	6	numeric	1.868	0.311	27	0.046	audio
medical	978	1,449	45	nominal	1.245	0.028	94	0.096	text
enron	1,702	1,001	53	nominal	3.378	0.064	753	0.442	text
image	2,000	294	5	numeric	1.236	0.247	20	0.010	image
scene	2.407	294	5	numeric	1.074	0.179	15	0.006	image
yeast	2.417	103	14	numeric	4.237	0.303	198	0.082	biology
slashdot	3,782	1,079	22	nominal	1.181	0.054	156	0.041	text
rcv1-s1	6,000	500	101	nominal	2.880	0.029	1,028	0.171	text
rcv1-s2	6,000	500	101	nominal	2.634	0.026	954	0.159	text
rcv1-s3	6,000	500	101	nominal	2.614	0.026	939	0.156	text
rcv1-s4	6,000	500	101	nominal	2.484	0.025	816	0.136	text
bibtex	7395	1836	159	nominal	2.402	0.015	2856	0.386	text
corel16k (sample 1)	13766	500	153	nominal	2.859	0.019	4803	0.349	image
corel16k (sample 2)	13761	500	153	nominal	2.882	0.018	4868	0.354	image

by enriching the base label-specific features of each class label via synergizing informative label-specific features from other class labels with sparse regularization (Steps 5-8). In this way, full-order label correlations have been considered via the synergy process of base label-specific features from all class labels. After that, a number of binary classifiers are generated based on the generated label-specific features (Steps 9-12) and then employed to make prediction on unseen instance (Steps 13-15).

4. Experiments

4.1. Experimental Setup

Table 2 summarizes detailed characteristics of the fifteen benchmark multi-label data sets employed for experimental studies. For each multi-label data set $\mathcal{S}$, we use $|\mathcal{S}|$, $dim(\mathcal{S})$, $L(\mathcal{S})$ and $F(\mathcal{S})$ to represent the number of examples, number of features, number of class labels and feature type respectively. In addition, several multi-label statistics including label cardinality $LCard(\mathcal{S})$, label density $LDen(\mathcal{S})$, distinct label sets $DL(\mathcal{S})$ and proportion of distinct label sets $PDL(\mathcal{S})$ are also utilized to characterize properties of each data set. Detailed definitions on these multi-label statistics can be found in (Read et al., 2011; Zhan and Zhang, 2017).

As shown in Table 2, experimental data sets are roughly organized in ascending order of $|\mathcal{S}|$ with eight being regular-scale (first part, $|\mathcal{S}| < 5,000$) and seven being large-scale (second part, $|\mathcal{S}| \geq 5,000$). Specifically, the fifteen experimental data sets exhibit diversified multi-label properties which provide solid basis for thorough comparative studies.

To show the effectiveness of the proposed REEL approach, five benchmark multi-label learning approaches have been employed for comparative studies (with parameter configuration suggested in respective literatures):

- BR (Boutell et al., 2004): A baseline approach which decomposes the multi-label learning problem into a number of independent binary learning problems, one per class label. BR employs the original feature representation for inducing all binary classifiers, which can be regarded as a degenerated version of label-specific features strategy. [Base learner: linear kernel SVM]

- MDDM (Zhang and Zhou, 2010): A multi-label dimensionality reduction approach which works by maximizing the dependence between original feature space and the associated class labels. [$thr = 99\%$]

- LIFT (Zhang and Wu, 2015): A first-order multi-label learning approach based on label-specific features strategy, which generates tailored features via conducting clustering analysis on each class label independently. [Base learner: linear kernel SVM, $r = 0.1$]

- LLSF (Huang et al., 2016): A second-order multi-label learning approach based on label-specific features strategy, which generates tailored features by retaining a different subset of original features for each class label with feature-sharing between a pair of closely-related class labels. [$\alpha = 0.5$, $\beta = 0.1$, $\gamma = 0.01$]

- MLSF (Sun et al., 2016): A high-order multi-label learning approach based on label-specific features strategy, which generates tailored features by retaining a different subset of original features for a group of class labels. [$K = \lceil q/10 \rceil$, $\epsilon = 0.01$, $\alpha = 0.8$, $\gamma = 0.01$, $\rho = 1$]

For each comparing approach, parameter setup is stated above, which is suggested in respective literature. For REEL, as shown in Table 1, the regularization parameter λ is set to be 1 and Libsvm (Chang and Lin, 2011) is employed to instantiate the binary learning algorithm $\mathcal{L}$.

To evaluate the performance of each comparing approach, six widely-used multi-label evaluation metrics are used including *hamming loss*, *ranking loss*, *one-error*, *coverage*, *average precision* and *micro-averaging AUC* (Zhang and Zhou, 2014).[2] For the first four metrics, the smaller the metric value the better the performance. For the other two metrics, the larger the metric value the better the performance. Ten-fold cross-validation is performed on each benchmark data set, where the mean metric value as well as standard deviation are recorded for performance evaluation.

4.2. Experimental Results

Tables 3 to 8 report the detailed experimental results of each comparing approach in terms of each evaluation metric respectively. Furthermore, the best performance among the comparing approaches is also shown in boldface. In this paper, Friedman test (Demšar, 2006) is employed here for statistical performance comparisons of multiple algorithms over a number of data sets. It is shown that at significance level $\alpha = 0.05$, the null hypothesis of equal performance among the comparing approaches is rejected in terms of each evaluation metric. Consequently, *Bonferroni-Dunn test* (Demšar, 2006) is employed as the post-hoc test to show the relative performance among comparing approaches by treating REEL as the control approach.

Figure 1 illustrates the CD diagrams where the average rank of each approach is marked along the axis with lower ranks to the right. Any approach whose average rank is within one critical

[2] All evaluation metrics take value in [0,1], where *coverage* is normalized by the number of class labels.

Table 3: The performance of each comparing approach (mean ± std. deviation) on each data set in terms of *hamming loss*. On each data set, the best performance among the comparing algorithms is shown in bold face.

Dataset	Reel	Br	Mddm	Lift	Llsf	Mlsf
CAL500	**0.137±0.005**	0.215±0.016	0.140±0.004	0.138±0.004	0.166±0.078	0.138±0.004
emotions	**0.178±0.019**	0.318±0.0635	0.394±0.028	0.179±0.015	0.184±0.005	0.407±0.021
medical	**0.012±0.001**	0.019±0.0.001	0.017±0.002	0.022±0.008	0.025±0.002	0.013±0.002
enron	**0.048±0.002**	0.060±0.003	0.052±0.001	0.075±0.002	0.089±0.003	0.052±0.002
image	**0.154±0.009**	0.179±0.011	0.191±0.008	0.156±0.009	0.184±0.013	0.223±0.014
scene	**0.076±0.009**	0.110±0.007	0.437±0.019	0.080±0.009	0.144±0.012	0.126±0.008
yeast	**0.191±0.004**	0.200±0.008	0.199±0.005	0.197±0.005	0.311±0.009	0.209±0.006
slashdot	0.039±0.002	0.049±0.002	0.038±0.002	**0.037±0.008**	0.042±0.002	0.044±0.001
rcv1-s1	**0.026±0.001**	0.034±0.001	0.027±0.001	0.028±0.001	0.030±0.001	0.028±0.001
rcv1-s2	**0.023±0.001**	0.031±0.001	0.024±0.001	**0.023±0.001**	0.025±0.001	0.024±0.001
rcv1-s3	**0.023±0.001**	0.031±0.001	0.024±0.001	**0.023±0.001**	0.025±0.001	0.024±0.001
rcv1-s4	**0.019±0.001**	0.023±0.001	0.020±0.001	0.020±0.001	0.022±0.001	**0.019±0.001**
bibtex	**0.078±0.006**	0.084±0.001	0.104±0.006	0.082±0.007	0.082±0.007	0.350±0.023
corel16k-s1	0.164±0.004	0.220±0.001	0.185±0.007	**0.162±0.003**	0.170±0.006	0.177±0.003
corel16k-s2	0.172±0.002	0.224±0.001	0.184±0.011	0.172±0.003	**0.166±0.007**	0.169±0.005

Table 4: The performance of each comparing approach (mean ± std. deviation) on each data set in terms of *ranking loss*. On each data set, the best performance among the comparing algorithms is shown in bold face.

Dataset	Reel	Br	Mddm	Lift	Llsf	Mlsf
CAL500	**0.137±0.005**	0.215±0.016	0.140±0.004	0.138±0.004	0.166±0.078	0.138±0.004
emotions	0.138±0.021	**0.113±0.047**	0.479±0.044	0.144±0.023	0.258±0.031	0.483±0.042
medical	0.036±0.014	0.041±0.001	**0.027±0.010**	0.053±0.016	0.046±0.028	0.050±0.035
enron	0.084±0.005	**0.016±0.001**	0.097±0.006	0.219±0.004	0.126±0.005	0.089±0.003
image	**0.154±0.009**	0.179±0.011	0.191±0.008	0.156±0.009	0.184±0.013	0.223±0.014
scene	0.062±0.007	**0.030±0.029**	0.437±0.019	0.061±0.008	0.097±0.016	0.125±0.011
yeast	0.164±0.008	**0.058±0.006**	0.175±0.007	0.165±0.006	0.357±0.014	0.209±0.009
slashdot	0.403±0.035	0.508±0.024	**0.357±0.023**	0.363±0.015	0.380±0.022	0.476±0.022
rcv1-s1	**0.050±0.003**	0.071±0.001	0.089±0.005	0.053±0.003	0.060±0.03	0.074±0.004
rcv1-s2	**0.053±0.003**	0.060±0.001	0.089±0.004	0.058±0.002	0.062±0.005	0.080±0.004
rcv1-s3	**0.053±0.002**	0.065±0.001	0.097±0.004	0.058±0.003	0.059±0.003	0.083±0.006
rcv1-s4	**0.037±0.002**	0.057±0.001	0.067±0.005	0.040±0.003	0.050±0.005	0.057±0.006
bibtex	**0.078±0.006**	0.084±0.001	0.104±0.006	0.082±0.007	0.082±0.007	0.350±0.023
corel16k-s1	0.164±0.004	0.220±0.001	0.185±0.007	**0.162±0.003**	0.170±0.006	0.177±0.003
corel16k-s2	0.172±0.002	0.224±0.001	0.184±0.011	0.172±0.003	**0.166±0.007**	0.69±0.005

difference (CD) with Reel is interconnected to each other with a thick line. Otherwise, it is regarded to have significantly different performance against Reel.

Based on the reported experimental results, the following major observations can be made:

Table 5: The performance of each comparing approach (mean ± std. deviation) on each data set in terms of *one-error*. On each data set, the best performance among the comparing algorithms is shown in bold face.

Dataset	REEL	BR	MDDM	LIFT	LLSF	MLSF
CAL500	**0.119±0.043**	0.515±0.207	0.209±0.020	0.129±0.057	0.127±0.009	0.124±0.044
emotions	**0.237±0.051**	0.544±0.100	0.659±0.068	0.238±0.073	0.424±0.063	0.676±0.041
medical	**0.163±0.024**	0.181±0.035	0.230±0.041	0.347±0.059	0.213±0.028	0.184±0.031
enron	0.249±0.025	0.418±0.034	0.290±0.054	**0.235±0.029**	0.255±0.016	0.299±0.028
image	0.262±0.025	0.410±0.032	0.345±0.022	**0.258±0.029**	0.322±0.023	0.458±0.032
scene	**0.190±0.026**	0.337±0.033	0.437±0.019	0.191±0.026	0.263±0.031	0.343±0.030
yeast	**0.216±0.023**	0.336±0.038	0.232±0.030	0.224±0.016	0.373±0.026	0.253±0.029
slashdot	0.403±0.035	0.508±0.024	**0.357±0.023**	0.363±0.015	0.380±0.022	0.476±0.022
rcv1-s1	0.421±0.019	0.640±0.018	0.474±0.035	**0.420±0.013**	0.421±0.019	0.500±0.012
rcv1-s2	**0.429±0.017**	0.590±0.014	0.483±0.027	0.433±0.019	0.488±0.012	0.509±0.011
rcv1-s3	0.442±0.002	0.592±0.013	0.487±0.026	0.450±0.003	**0.413±0.011**	0.450±0.003
rcv1-s4	0.387±0.013	0.458±0.017	0.443±0.053	0.385±0.010	0.341±0.017	**0.362±0.008**
bibtex	0.391±0.015	0.547±0.022	0.460±0.081	0.413±0.010	**0.347±0.021**	0.350±0.023
corel16k-s1	0.699±0.019	0.878±0.009	0.728±0.024	0.680±0.023	**0.638±0.009**	0.781±0.024
corel16k-s2	0.655±0.007	0.880±0.007	0.736±0.018	0.667±0.005	**0.638±0.012**	0.766±0.020

Table 6: The performance of each comparing approach (mean ± std. deviation) on each data set in terms of *coverage*. On each data set, the best performance among the comparing algorithms is shown in bold face.

Dataset	REEL	BR	MDDM	LIFT	LLSF	MLSF
CAL500	0.758±0.016	0.976±0.007	0.754±0.012	0.761±0.015	**0.742±0.028**	0.795±0.021
emotions	**0.279±0.026**	0.485±0.059	0.523±0.033	0.283±0.021	0.376±0.037	0.529±0.040
medical	**0.052±0.015**	0.120±0.025	0.055±0.015	0.072±0.019	0.088±0.018	0.069±0.037
enron	**0.237±0.009**	0.585±0.020	0.261±0.011	0.219±0.009	0.265±0.008	0.239±0.007
image	**0.167±0.011**	0.270±0.015	0.199±0.010	0.168±0.013	0.195±0.013	0.242±0.017
scene	0.066±0.007	0.163±0.016	0.437±0.019	**0.065±0.008**	0.096±0.015	0.119±0.010
yeast	**0.454±0.008**	0.637±0.017	0.462±0.007	0.454±0.007	0.630±0.011	0.516±0.008
slashdot	0.103±0.009	0.224±0.012	**0.087±0.006**	0.093±0.007	0.134±0.006	0.123±0.005
rcv1-s1	**0.124±0.008**	0.449±0.013	0.200±0.008	0.126±0.008	0.139±0.007	0.169±0.008
rcv1-s2	**0.127±0.007**	0.378±0.009	0.192±0.008	0.136±0.005	0.139±0.010	0.173±0.009
rcv1-s3	0.124±0.005	0.380±0.010	0.209±0.008	**0.119±0.008**	0.133±0.005	0.183±0.039
rcv1-s4	**0.090±0.003**	0.330±0.013	0.145±0.008	0.093±0.004	0.112±0.009	0.130±0.019
bibtex	0.145±0.011	0.439±0.008	0.184±0.009	**0.142±0.013**	0.151±0.007	0.350±0.023
corel16k-s1	0.323±0.007	0.670±0.008	0.364±0.015	0.328±0.004	**0.312±0.009**	0.344±0.005
corel16k-s2	0.320±0.015	0.668±0.006	0.364±0.021	0.312±0.013	**0.308±0.011**	0.334±0.008

- It is impressive that REEL achieves lowest average rank in terms of all evaluation metrics. No comparing approach has significantly outperformed REEL based on the Friedman statistical test.

Table 7: The performance of each comparing approach (mean ± std. deviation) on each data set in terms of *average precision*. On each data set, the best performance among the comparing algorithms is shown in bold face.

Dataset	REEL	BR	MDDM	LIFT	LLSF	MLSF
CAL500	**0.503±0.012**	0.226±0.038	0.491±0.018	0.499±0.012	0.497±0.078	0.481±0.009
emotions	**0.826±0.051**	0.629±0.048	0.538±0.038	0.818±0.034	0.703±0.040	0.532±0.024
medical	**0.872±0.015**	0.809±0.035	0.837±0.031	0.742±0.038	0.789±0.022	0.849±0.027
enron	0.672±0.019	0.457±0.020	0.626±0.023	**0.697±0.010**	0.665±0.016	0.642±0.013
image	**0.828±0.013**	0.722±0.012	0.778±0.012	0.826±0.016	0.790±0.015	0.709±0.019
scene	**0.887±0.014**	0.768±0.018	0.437±0.019	0.883±0.014	0.839±0.020	0.791±0.018
yeast	**0.770±0.015**	0.675±0.016	0.754±0.015	0.766±0.015	0.602±0.015	0.719±0.014
slashdot	0.695±0.024	0.592±0.021	**0.735±0.015**	0.711±0.013	0.707±0.012	0.637±0.016
rcv1-s1	0.591±0.009	0.382±0.009	0.496±0.015	0.585±0.010	**0.607±0.008**	0.511±0.008
rcv1-s2	0.606±0.008	0.433±0.012	0.516±0.018	0.600±0.009	**0.627±0.012**	0.520±0.036
rcv1-s3	0.601±0.010	0.437±0.015	0.506±0.016	0.596±0.012	**0.625±0.008**	0.561±0.015
rcv1-s4	0.667±0.009	0.489±0.017	0.572±0.029	0.658±0.008	**0.698±0.012**	0.655±0.011
bibtex	0.550±0.013	0.386±0.029	0.483±0.031	0.545±0.011	**0.603±0.013**	0.350±0.023
corel16k-s1	0.301±0.009	0.104±0.003	0.274±0.007	**0.305±0.010**	0.156±0.029	0.255±0.010
corel16k-s2	0.312±0.005	0.096±0.003	0.264±0.009	0.318±0.008	**0.341±0.008**	0.255±0.006

Table 8: The performance of each comparing approach (mean ± std. deviation) on each data set in terms of *macro-averaging AUC*. On each data set, the best performance among the comparing algorithms is shown in bold face.

Dataset	REEL	BR	MDDM	LIFT	LLSF	MLSF
CAL500	0.554±0.012	0.501±0.001	0.517±0.018	0.546±0.010	**0.566±0.016**	0.519±0.012
emotions	**0.858±0.023**	0.594±0.033	0.488±0.048	**0.858±0.016**	0.553±0.032	0.486±0.038
medical	**0.894±0.052**	0.808±0.034	0.878±0.025	0.863±0.042	0.825±0.033	0.888±0.039
enron	0.683±0.020	0.595±0.015	**0.684±0.036**	0.731±0.022	0.675±0.023	0.674±0.020
image	**0.860±0.012**	0.717±0.012	0.815±0.015	**0.860±0.014**	0.788±0.023	0.778±0.025
scene	**0.948±0.006**	0.801±0.017	0.437±0.019	0.945±0.007	0.922±0.011	0.888±0.009
yeast	0.686±0.015	0.572±0.008	0.614±0.015	**0.693±0.019**	0.566±0.016	0.616±0.013
slashdot	0.853±0.012	0.682±0.013	**0.881±0.015**	0.861±0.017	0.850±0.011	0.819±0.015
rcv1-s1	**0.912±0.004**	0.900±0.001	0.899±0.006	0.911±0.009	0.903±0.004	0.672±0.009
rcv1-s2	**0.900±0.001**	0.617±0.011	0.825±0.016	0.892±0.007	0.857±0.006	0.835±0.008
rcv1-s3	**0.899±0.006**	0.616±0.009	0.779±0.025	0.886±0.008	0.852±0.008	0.842±0.009
rcv1-s4	**0.911±0.009**	0.621±0.007	0.810±0.021	0.905±0.049	0.833±0.012	0.746±0.028
bibtex	0.903±0.004	0.648±0.007	0.887±0.005	**0.908±0.003**	0.898±0.009	0.350±0.023
corel16k-s1	0.672±0.009	0.520±0.003	0.622±0.011	**0.678±0.010**	**0.678±0.009**	0.661±0.008
corel16k-s2	0.719±0.009	0.522±0.004	0.628±0.011	**0.720±0.008**	0.709±0.007	0.676±0.008

- Compared to BR which corresponds to the degenerated version of label-specific features strategy without considering tailored features for each class label, REEL achieves superior performance in terms of all evaluation metrics except *ranking loss*.

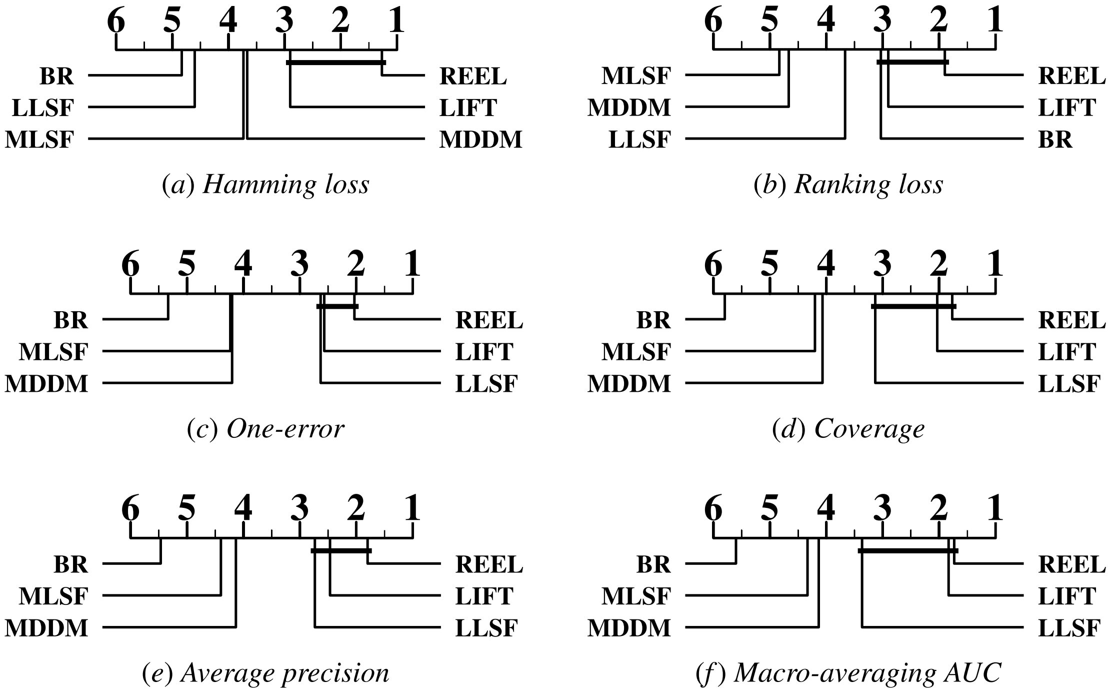

(*a*) *Hamming loss*

(*b*) *Ranking loss*

(*c*) *One-error*

(*d*) *Coverage*

(*e*) *Average precision*

(*f*) *Macro-averaging AUC*

Figure 1: Comparison of REEL (control approach) against other approaches with the *Bonferroni-Dunn test*. Approaches not connected with REEL in the CD diagram are considered to have significantly different performance from the control approach (CD=1.7597 at 0.05 significance level).

- Compared to MDDM which performs feature manipulation via dimensionality reduction, REEL achieves superior performance in terms of all evaluation metrics.

- Compared to other learning approaches LIFT, LLSF and MLSF which also employs the strategy of label-specific features for model induction, REEL achieves superior performance in 63.3% cases out of 30 statistical comparisons (5 comparing approaches × 6 evaluation metrics).

As shown in Table 1, two parameters λ and $\mathcal{L}$ need to be specified to instantiate REEL. In this paper, SVM is utilized to serve as the binary learning algorithm $\mathcal{L}$. For the other regularization parameter λ, Figure 2 shows how the performance of REEL changes as the value of λ increases in terms of several evaluation metrics. Generally, the performance of REEL is relatively stable with λ taking values within [0.1, 1]. In this paper, λ is set to be 1 as shown in Subsection 4.1.

5. Conclusion

In this paper, the problem of generating label-specific features for multi-label learning is studied. By employing a two-stage generation procedure, the base label-specific features for each class label are enriched by concatenating informative label-specific features from other class labels via sparse regularization. The computational complexity of resulting multi-label classification model is linear to the number of class labels in label space. Comprehensive comparative studies against state-

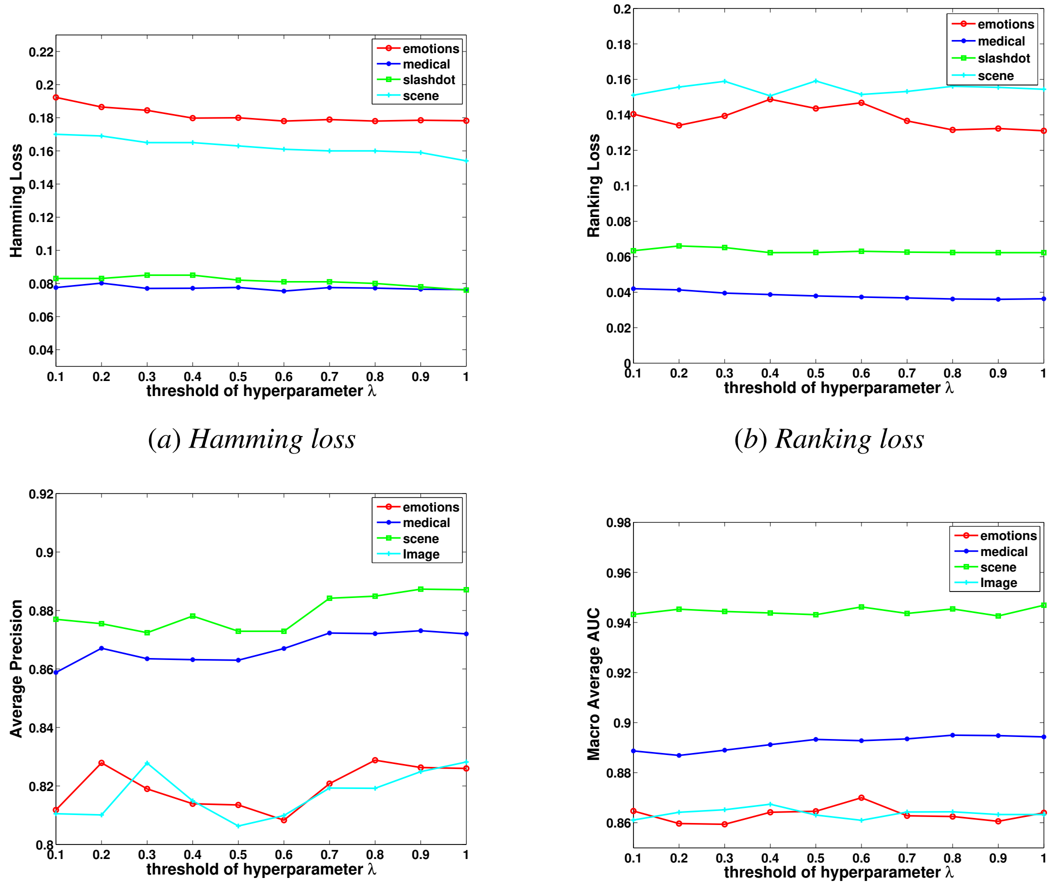

(*a*) *Hamming loss*

(*b*) *Ranking loss*

(*c*) *Average precision*

(*d*) *Macro-averaging AUC*

Figure 2: The performance of REEL changes as the value of parameter λ increases.

of-the-art approaches validate the effectiveness of the proposed label-specific features generation techniques for multi-label learning.

Acknowledgements

The authors wish to thank the anonymous reviewers for their helpful comments and suggestions. This work was supported by the National Key R&D Program of China (2018YFB1004300), the National Science Foundation of China (61573104), and partially supported by the Collaborative Innovation Center of Novel Software Technology and Industrialization.

References

M. Boutell, J. Luo, X. Shen, and C. M. Brown. Learning multi-label scene classification. *Pattern Recognition*, 37(9):1757–1771, 2004.

C. Brinker, E. Loza Mencía, and J. Fürnkranz. Graded multilabel classification by pairwise comparisons. In *Proceedings of the 14th IEEE International Conference on Data Mining*, pages 731–736, Shenzhen, China, 2014.

S. Canuto, M. A. Gonçalves, and F. Benevenuto. Exploiting new sentiment-based meta-level features for effective sentiment analysis. In *Proceedings of the 9th ACM International Conference on Web Search and Data Mining*, pages 53–62, San Francisco, CA, 2016.

C.-C Chang and C.-J. Lin. LIBSVM: A library for support vector machines. *ACM Transactions on Intelligent Systems and Technology*, 2:27:1–27:27, 2011. Software available at http://www.csie.ntu.edu.tw/~cjlin/libsvm.

J. Demšar. Statistical comparisons of classifiers over multiple data sets. *Journal of Machine Learning Research*, 7(1):1–30, 2006.

J. Fürnkranz, E. Hüllermeier, E. Loza Mencía, and K. Brinker. Multilabel classification via calibrated label ranking. *Machine Learning*, 73(2):133–153, 2008.

E. Gibaja and S. Ventura. A tutorial on multilabel learning. *ACM Computing Surveys*, 47(3):Article 52, 2015.

J. Huang, G. Li, Q. Huang, and X. Wu. Learning label-specific features and class-dependent labels for multi-label classification. *IEEE Transactions on Knowledge and Data Engineering*, 28(12): 3309–3323, 2016.

J. Huang, G. Li, Q. Huang, and X. Wu. Joint feature selection and classification for multilabel learning. *IEEE Transactions on Cybernetics*, 48(3):876–889, 2018.

X. Pan, Y.-X. Fan, J. Jia, and H.-B. Shen. Identifying rna-binding proteins using multi-label deep learning. *Science China Information Sciences*, page 62:19103, 2019.

R. B. Pereira, A. Plastino, B. Zadrozny, and L. H. C. Merschmann. Categorizing feature selection methods for multi-label classification. *Artificial Intelligence Review*, 49(1):57–78, 2018.

J. Read, B. Pfahringer, G. Holmes, and E. Frank. Classifier chains for multi-label classification. *Machine Learning*, 85(3):333–359, 2011.

T. N. Rubin, A. Chambers, P. Smyth, and M. Steyvers. Statistical topic models for multi-label document classification. *Machine Learning*, 88(1-2):157–208, 2012.

F. Sun, J. Tang, H. Li, G.-J. Qi, and T. S. Huang. Multi-label image categorization with sparse factor representation. *IEEE Transactions on Image Processing*, 23(3):1028–1037, 2014.

L. Sun, S. Ji, and J. Ye. *Multi-label Dimensionality Reduction*. Chapman and Hall/CRC, Boca Ration, FL, 2013.

L. Sun, M. Kudo, and K. Kimura. Multi-label classification with meta-label-specific features. In *Proceedings of the 23rd International Conference on Pattern Recognition*, pages 1612–1617, Cancun, Mexico, 2016.

K. Trohidis, G. Tsoumakas, G. Kalliris, and I. Vlahavas. Multi-label classification of music by emotion. *EURASIP Journal on Audio, Speech, and Music Processing*, 2011.

G. Tsoumakas, I. Katakis, and I. Vlahavas. Random k-labelsets for multi-label classification. *IEEE Transactions on Knowledge and Data Engineering*, 23(7):1079–1089, 2011.

X. Wang and G. Sukthankar. Multi-label relational neighbor classification using social context features. In *Proceedings of the 19th ACM SIGKDD International Conference on Knowledge Discovery and Data Mining*, pages 464–472, Chicago, IL, 2013.

W. Weng, Y. Lin, S. Wu, Y. Li, and Y. Kang. Multi-label learning based on label-specific features and local pairwise label correlation. *Neurocomputing*, 273:385–394, 2018.

B. Wu, E. Zhong, A. Horner, and Q. Yang. Music emotion recognition by multi-label multi-layer multi-instance multi-view learning. In *Proceedings of the 22nd ACM International Conference on Multimedia*, pages 117–126, Orlando, FL, 2014.

S. Xu, X. Yang, H. Yu, D.-J. Yu, J. Yang, and E. C. C. Tsang. Multi-label learning with label-specific feature reduction. *Knowledge-Based Systems*, 104:52–61, 2016.

Y. Yang and S. Gopal. Multilabel classification with meta-level features in a learning-to-rank framework. *Machine Learning*, 88(1-2):47–68, 2012.

W. Zhan and M.-L. Zhang. Inductive semi-supervised multi-label learning with co-training. In *Proceedings of the 23rd ACM SIGKDD Conference on Knowledge Discovery and Data Mining*, pages 1305–1314, Halifax, Canada, 2017.

C. Zhang, Z. Yu, Q. Hu, P. Zhu, X. Liu, and X. Wang. Latent semantic aware multi-view multi-label classification. In *Proceedings of the 32nd AAAI Conference on Artificial Intelligence*, pages 4414–4421, New Orleans, LA, 2018a.

J. Zhang, C. Li, D. Cao, Y. Lin, S. Su, L. Dai, and S. Li. Multi-label learning with label-specific features by resolving label correlations. *Knowledge-Based Systems*, 159:148–157, 2018b.

M.-L. Zhang and L. Wu. LIFT: Multi-label learning with label-specific features. *IEEE Transactions on Pattern Analysis and Machine Intelligence*, 37(1):107–120, 2015.

M.-L. Zhang and Z.-H. Zhou. A review on multi-label learning algorithms. *IEEE Transactions on Knowledge and Data Engineering*, 26(8):1819–1837, 2014.

M.-L. Zhang, Y.-K. Li, Y.-Y. Liu, and X. Geng. Binary relevance for multi-label learning: An overview. *Frontiers of Computer Science*, 12(2):191–202, 2018c.

Y. Zhang and Z.-H. Zhou. Multilabel dimensionality reduction via dependence maximization. *ACM Transactions on Knowledge Discovery from Data*, 4(3):Article 14, 2010.

X. Zhu, X. Li, and S. Zhang. Block-row sparse multiview multilabel learning for image classification. *IEEE Transactions on Cybernetics*, 46(2):450–461, 2016.